PROCEEDINGS B

royalsocietypublishing.org/journal/rspb

Research

Cite this article: Xiao M, Burford MA, Prentice MJ, Galvanese EF, Chuang A, Hamilton DP. 2023 Phosphorus storage and utilization strategies of two bloom-forming freshwater cyanobacteria. *Proc. R. Soc. B* **290**: 20231204. https://doi.org/10.1098/rspb.2023.1204

Received: 31 May 2023
Accepted: 22 June 2023

Subject Category:
Development and physiology

Subject Areas:
physiology, ecology, microbiology

Keywords:
alkaline phosphatase activity (APA), cellular P quota, intra-population variation, Michaelis–Menten kinetics, nutrient uptake affinity, nutrient limitation

Author for correspondence:
Man Xiao
e-mail: mxiao@niglas.ac.cn

Electronic supplementary material is available online at https://doi.org/10.6084/m9.figshare.c.6729669.

THE ROYAL SOCIETY PUBLISHING

Phosphorus storage and utilization strategies of two bloom-forming freshwater cyanobacteria

Man Xiao[1,2], Michele A. Burford[2], Matthew J. Prentice[2,3], Elena F. Galvanese[4,5], Ann Chuang[2] and David P. Hamilton[2]

[1]State Key Laboratory of Lake Science and Environment, Nanjing Institute of Geography and Limnology, Chinese Academy of Sciences, Nanjing 210008, People's Republic of China
[2]Australian Rivers Institute, Griffith University, 170 Kessels Road, Nathan, QLD 4111, Australia
[3]Environmental Research Institute, The University of Waikato, Hamilton 3240, New Zealand
[4]Laboratório de Análise e Síntese em Biodiversidade, Departamento de Botânica, Setor de Ciências Biológicas, Universidade Federal do Paraná, Curitiba, PR 81531-980, Brazil
[5]Programa de Pós-graduação em Ecologia e Conservação, Setor de Ciências Biológicas, Universidade Federal do Paraná, Curitiba PR 80060-140, Brazil

MX, 0000-0003-0021-2129; MAB, 0000-0002-1076-6144; MJP, 0000-0001-5563-2046; EFG, 0000-0002-9956-314X; AC, 0000-0002-8344-2765; DPH, 0000-0002-9341-8777

The inter-relationships between cellular phosphorus (P) storage, dissolved inorganic P (DIP) uptake affinity, alkaline phosphatase activity (APA) and dissolved inorganic nitrogen (DIN) concentrations were studied in two ubiquitous diazotrophic freshwater cyanobacteria, *Raphidiopsis raciborskii* (six strains) and *Chrysosporum ovalisporum* (two strains). DIP uptake kinetics were measured using rates of incorporation of the radio-isotope, ^{33}P and APA as a proxy for DOP-ester utilization. The study showed that DIP uptake of individual strains followed Michaelis–Menten kinetics (modified in our study to incorporate cellular P quotas), but differed with DIN and P availability, and between growth stages. High-affinity DIP uptake and APA were activated below a P quota threshold of approximately 0.01 µg P µg^{-1} C across the species and strains. *C. ovalisporum* had significantly higher APA and P quotas (per unit C and cell) but lower uptake affinity than *R. raciborskii*. Demand for DIP by *C. ovalisporum* increased when N fixation occurred, but typically not for *R. raciborskii*. Our results indicate that cyanobacterial species and strains differ in their strategies to P limiting conditions, and highlight the interplay between N and P. Physiological adaptations like APA and diazotrophy of cyanobacteria adapting to low DIP and/or DIN conditions may occur simultaneously and drive species dominance in oligotrophic environments.

1. Background

Lake eutrophication and associated increases in toxic cyanobacterial blooms have had significant ecosystem impacts and been a major area of research over several decades [1]. Despite ongoing research on nutrient impacts on cyanobacteria bloom formation, our understanding of nutrient–cyanobacteria interactions remains simplistic [2]. Cyanobacteria blooms can persist even when dissolved inorganic phosphorus (DIP) concentrations are below standard analytical detection limits [3,4]. Physiological studies have demonstrated that cyanobacterial species possess a suite of P utilization strategies that promote bloom formation and resilience under low and/or fluctuating P conditions [5,6]. Information on the variety of strategies used by cyanobacteria to maintain dominance and form blooms under low-nutrient conditions is critical for predicting biomass as well as species composition.

The harmful cyanobacterium *Raphidiopsis raciborskii* (basionym *Cylindrospermopsis raciborskii*) is reported to be the dominant species in more than 18% of

freshwater cyanobacterial blooms globally [7]. Many lakes and reservoirs with *R. raciborskii* blooms have low DIP concentrations [8,9]. The dominance of *R. raciborskii* has been, in part, attributed to its ability to switch from passive (low-affinity) to active (high-affinity) DIP uptake at low concentrations of external DIP, i.e. approximately 5 µg P l^{-1} [10]. Most conventional models that simulate nutrient uptake rates, e.g. based on Michaelis–Menten kinetics, use external DIP, not cellular P quota, and therefore do not capture the observed plasticity of DIP uptake [11]. The addition of cellular P quotas is proposed as a mechanism to address this plasticity and capture the nutrient history that moderates DIP uptake rates [5]. However, there is limited information on how the cellular P quota drives uptake affinity, and on transitions between passive and active DIP uptake.

Cell storage of P is another strategy for dealing with low DIP. Cellular P quotas can vary fourfold among *R. raciborskii* strains isolated from the same population and are significantly higher in DIN-free treatments than those in replete DIN and P treatments [12]. However, the interplay between P quota, and DIP uptake affinity across strains and species remains poorly understood.

Organic P is the dominant form of P in most freshwater systems, with dissolved organic P (DOP) typically constituting 25–50% of the total P pool [13]. Simple forms of DOP, particularly esters, are a potential P source for growth and metabolism of many phytoplankton species, e.g. *R. raciborskii* [14,15]. Another bloom-forming cyanobacterium, *Chrysosporum ovalisporum* (basionym *Aphanizomenon ovalisporum*), is also considered to have high capacity for DOP utilization [16]. However, direct comparisons of DOP utilization and the interplay with DIP uptake among species are very limited.

All the strategies outlined above to access P during low DIP conditions are energy intensive and require sufficient N [17]. While both *C. ovalisporum* and *R. raciborskii* are N fixers, there are also energetic costs in fixing N. Previous studies have shown faster growth rates and little or no fixation when DIN is available. Therefore, it can be assumed that DIN limitation will also affect the capacity of these species to use high-affinity DIP uptake, APA and ultimately P storage. However, this inter-relationship between N and P has received little attention in previous studies [18].

Therefore, in this study, we compared DIP uptake kinetics and APA (as a proxy for DOP-ester utilization), between six and two strains, respectively, of the N_2-fixing cyanobacteria, *R. raciborskii* and *C. ovalisporum*. We hypothesized that the stoichiometry of N and P cell quotas and immediate growth requirements drive strategies for uptake and utilization of P. We tested our hypothesis using treatments and physiological assays designed to stimulate responses to DIP limitation, and both DIN and DIP limitation. These differences in P utilization may provide strategies to aid competition under different P and N conditions, and as a result would have a critical role in selecting the 'winners and losers' among species and strains.

2. Methods

Laboratory culture experiments were carried out with six *R. raciborskii* strains and two *C. ovalisporum* strains, under three nutrient treatments. Growth rate, cell number and biovolume, cellular carbon (C), nitrogen (N) and phosphorus (P), and dissolved N and P were analysed. DIP uptake bioassays were conducted to compare uptake rate, and APA assays were conducted to compare the enzymatic conversion of P-esters into DIP. Analyses were run on specific days listed in electronic supplementary material, table S1 over the duration of the experiment for all strains.

(a) Experimental set-up

(i) Study species and strains

The six *R. raciborskii* strains, WS01, WS02, WS03, WS08, WS09 and WS11, noted as S01 – S11 in Xiao *et al.* [7], were isolated in 2013 from surface water samples from Lake Wivenhoe (27°23′38″S, 152°36′28″E, the largest drinking water reservoir in southeast Queensland, Australia). The two *C. ovalisporum* strains, LHC01 and LHC02, were isolated in 2017 from surface water samples of brackish (approx. 8 ms cm^{-1}) Lake Hugh Muntz (28°2′60″S, 153°24′54″E). The *R. raciborskii* and *C. ovalisporum* blooms occur regularly in lakes Wivenhoe and Hugh Muntz, respectively, with DIP concentrations of both lakes close to or below analytical detection limits (0.06 µmol P l^{-1}) during summer stratification [9,19].

(ii) Culture maintenance and preparation

The strains of *R. raciborskii* were maintained in batch monocultures with modified Jaworski Medium comprising 45 µmol l^{-1} of DIP and 941 µmol l^{-1} of DIN (replete DIN and P, noted as JM), following Willis *et al.* [20]. In the case of *C. ovalisporum*, strains were maintained in 90% of the JM medium and 10% seawater by volume. Cultures were non-axenic; however, excess heterotrophic bacteria were removed during routine filtration and washing between subculturing (less than 5% biovolume). Cultures of each strain maintained under the optimal light and temperature conditions, were filtered and adapted to an environment of either replete DIN and P, or DIN-free prior to commencing the growth experiments (see details in electronic supplementary material, methods S1, Culture maintenance and preparation).

(iii) Growth experiment

Cultures acclimated to replete DIN and P, and DIN-free environments were washed and resuspended three times in sterile NP-free medium and split into four replicates for the growth experiment comprising three nutrient treatments (figure 1). For *R. raciborskii*, the three treatments were replete DIN and P, P-free (941 µmol l^{-1} of DIN but no P added) and NP-free (JM media with no DIN or P added). The former two treatments were from the pre-adapted replete DIN and P, and the latter was from the pre-adapted DIN-free. The strains of *C. ovalisporum* were also subjected to the three nutrient treatments, but the JM media was replaced by the 10% seawater JM media.

All cultures were inoculated at an initial optical density at a wavelength of 750 nm (OD750) of 0.020 ± 0.002, approximately 3.96×10^5 to 12.76×10^5 cells ml^{-1}, depending on the strain (see electronic supplementary material, table S3 for correlation between OD750 and cell counts; $R^2 = 0.90$–0.98 for the eight strains). Cultures were gently shaken each day during the experiment.

The photosynthetic yield (F_v/F_m) was measured using a Phyto-PAM (Walz, Effeltrich, Germany) along the growth experiment. A 10% reduction of the photosynthetic yield on 2 consecutive days was used as a rapid indicator of cell stress from P starvation, as per our previous study on *R. raciborskii* strains [12]. We found that once the photosynthetic yield was reduced by 10% on 2 consecutive days, it either stabilized, i.e. stationary phase indicator, or continued to decrease, i.e. stationary or death phase indicator; hence, we assumed that cultures became physiological stressed [12]. This method was also validated in bioassays conducted with algal populations in the

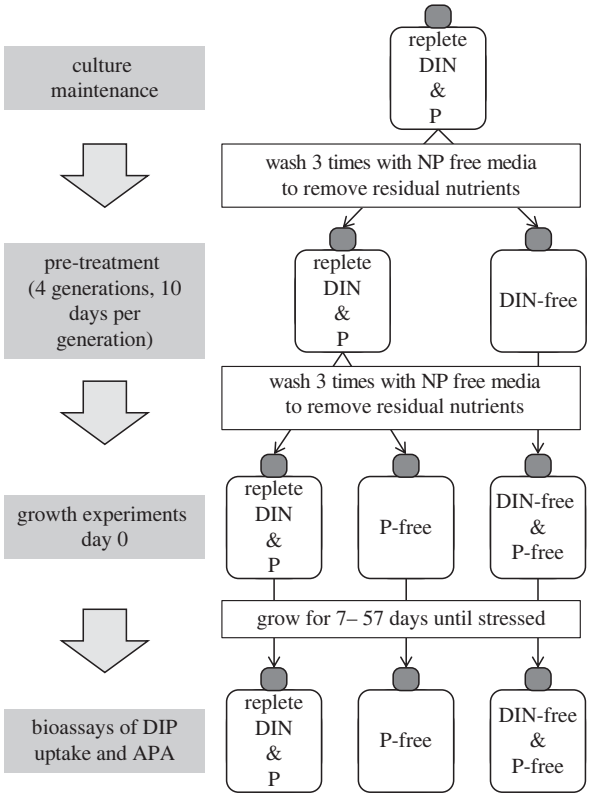

Figure 1. Schematic showing culture preparation, treatments, bioassays of DIP uptake and APA, for *R. raciborskii* and *C. ovalisporum* strains.

field [21]. We have shown that photosynthetic yield reduction occurred before stationary phase, hence photosynthetic yield, rather than spectrophotometric measures of optical densities of cultures, i.e. OD750, could more accurately indicate cell stress from nutrient limitation [12], minimizing the possibility of OD750 overestimating living cells and hence underestimating cellular P content. For *R. raciborskii* strains, the use of time to reach 10% reduction in photosynthetic yield as a measure was based on our previous experiments which used an identical set-up [12], and for *C. ovalisporum*, the time was calculated from F_v/F_m applying the same rule (see electronic supplementary material, figure S2).

(b) DIP uptake bioassay

(i) Pilot experiment

Pilot experiments were conducted (see electronic supplementary material, methods S2), and 11 DIP standard solutions (P1 through P11, see electronic supplementary material, table S2) with a decreasing total DIP concentration that comprised K_2HPO_4 (224.1 to 0.29 mg P l^{-1}, Chem-Supply, Australia) and labelled orthophosphoric acid $[^{33}P]H_3PO_4$ (34.7 pmol ml^{-1}, Biosci, Australia) were used for determining DIP uptake rates. Based on the pilot experiments, subsamples were taken at the following times after spiking DIP standard solutions into cultures: 10, 20, 30, 40 and 60 s for P-free and NP-free treatments, and 10 s, and 1, 2, 3, 5, 10, 20 min for the replete DIN and P treatment.

(ii) Bioassay set-up

Subcultures (duplicates) from each nutrient treatment were taken for DIP uptake bioassays when photosynthetic yield reduction occurred for all strains, and for *R. raciborskii* strains WS02 and WS09 from P-free and NP-free treatments during the exponential growth phase (day 7) (electronic supplementary material, table S1). For logistical reasons, DIP uptake kinetics was determined for four strains only: *R. raciborskii* WS02 and WS09, and *C. ovalisporum* LHC01 and LHC02, by spiking 8–10 labelled DIP solutions into subcultures (table 1). From the pilot experiments conducted with *R. raciborskii* WS02, we confirmed that the maximum or near-maximum uptake rates under both replete DIN and P, and the P-free treatments, were achieved by spiking solution P1 which had the highest DIP concentration. Hence, the maximum or near-maximum uptake rates for all strains were approximated by spiking solution P1.

In the bioassay, subsamples (7 ml) from each duplicate were placed in 50 ml polypropylene conical tubes and spiked with 7 to 14 µl of DIP standard solutions. The mixed solution resulted in DIP concentrations (S) ranging from 3.89×10^{-4} to 0.298 mg l^{-1}. One millilitre of the mixed solution was then gently filtered through a 0.4 µm polycarbonate membrane filter (Steritech, USA) at the time intervals described in the pilot experiment. The filter and filtrate (500 µl) were collected separately and placed in scintillation vials with 4 ml scintillation liquid that comprised 3.6 ml scintillation cocktail (Ultima Gold, PerkinElmer, VIC, Australia) and 0.4 ml MilliQ water. Mixtures were vortexed to completely mix. Background radioactivity was determined from the solution of scintillation liquid only. DIP standard solutions mixed with the scintillation liquid were also used as a reference to calculate the reading efficiency for each sample. All mixtures were read with a liquid scintillation counter (Tri-Carb 2810TR, PerkinElmer, MA, USA).

(iii) DIP uptake rate

The counts per minute (cpm) of all samples from the scintillation counter output were corrected with the reading efficiency and converted to disintegrations per minute (dpm) as a measure of radioactivity:

$$\mathrm{dpm} = \frac{\mathrm{cpm}}{\text{reading efficiency}}. \tag{2.1}$$

The *reading efficiency* of each subsample was calculated from comparing cpm readings of the combined filter and filtrate, to the cpm reading of the theoretical value, i.e. the spiked DIP standard solution:

$$\text{reading efficiency} = \frac{(\mathrm{cpm_{filter}} + \mathrm{cpm_{filtrate}})}{\mathrm{cpm_{standard}}}. \tag{2.2}$$

Phosphorus (P) incorporation into cyanobacteria cells, i.e. cells on the filter, was based on the dpm reading of the filter and the radioactivity and proportion of ^{33}P in the DIP solution:

$$\mathrm{dpm_{filter}} = \frac{\mathrm{cpm_{filter}}}{\text{reading efficiency}}, \tag{2.3}$$

and

$$\mathrm{P} = \frac{\mathrm{dpm_{filter}}}{2.2 \times 10^6} \cdot k \cdot \frac{1}{\%\ ^{33}P}, \tag{2.4}$$

where P is the amount of DIP that is taken up by cells (pmol), 2.2×10^6 is a constant of dpm in 1 µCi (radioactivity of ^{33}P), $\%\ ^{33}P$ is the percentage of ^{33}P in the DIP solution (electronic supplementary material, table S2), and k is pmol P in 1 µCi of the DIP standard solution. k is calculated from the amount of ^{33}P (pmol) and its real-time radioactivity, N_t (µCi), in the DIP standard solution. Here N_t is the radioactivity that undergoes decay after time t (d), calculated as follows:

$$N_t = N_0 e^{-0.693 \cdot t/25.6} \tag{2.5}$$

where N_0 is the original radioactivity (µCi) and 25.6 is the half-life of ^{33}P (d).

The uptake rate v (pmol P ml^{-1} min^{-1}) for each treatment over the time course T was then calculated from the changes of

Table 1. Average values of DIP uptake kinetics (*V*max, maximum uptake rate; *Ks*, half saturation constant; α, uptake affinity) that best fit a revised Michaelis–Menten equation for strains of *R. raciborskii* and *C. ovalisporum*, after running Monte Carlo simulations (see Methods). Day indicates the time to run the DIP uptake bioassay after culture inoculation.

species	strain	treatment	day (d)	DIP standard solutions	DIP uptake kinetics		
					V_{max} (µg P µg^{-1} C d^{-1})	K_v (mg l^{-1})	α (V_{max}/K_v)
Raphidiopsis raciborskii	WS02	replete DIN and P	18	1, 2, 3, 5, 6, 7, 9, 10	0.90	1.04	0.87
		P-free	7	1, 2, 3, 4, 5, 6, 7, 8, 9, 11	1.32	0.01	197.19
		P-free	14	3, 4, 5, 6, 7, 8, 9, 11	1.37	0.02	63.55
		NP-free	7	1, 2, 3, 5, 6, 7, 8, 9, 10, 11	1.23	0.03	40.11
		NP-free	14	3, 5, 6, 7, 8, 9, 10, 11	1.38	0.01	99.36
	WS09	replete DIN and P	14	1, 2, 3, 5, 6, 7, 9, 10	0.41	0.52	0.79
		P-free	7	3, 4, 5, 6, 7, 8, 9, 11	2.48	0.10	23.96
		P-free	10	3, 4, 5, 6, 7, 8, 9, 11	2.43	0.02	131.43
		NP-free	7	3, 4, 5, 6, 7, 8, 9, 11	1.16	0.06	17.94
		NP-free	14	3, 4, 5, 6, 7, 8, 9, 11	2.05	0.08	25.07
Chrysosporum ovalisporum	LHC01	replete DIN and P	57	1, 2, 3, 5, 6, 7, 10, 11	0.51	0.02	24.24
		P-free	55	1, 2, 3, 4, 5, 6, 7, 8, 9, 10	0.63	0.01	94.33
		NP-free	21	1, 2, 3, 4, 5, 6, 7, 8, 9, 10	0.76	0.01	110.66
	LHC02	replete DIN and P	53	2, 3, 4, 5, 6, 8, 9, 10	0.47	0.01	39.31
		P-free	54	2, 3, 4, 5, 6, 7, 8, 9, 10	0.56	0.01	69.87
		NP-free	14	1, 2, 3, 4, 5, 6, 7, 8, 9, 10	0.56	0.01	106.16

P concentration in each 1 ml filtrate in the bioassay:

$$v = \frac{\Delta[P]/\Delta T}{V}, \tag{2.6}$$

where $\Delta[P]$ is the change in P concentration (mg l^{-1}), ΔT is change in time (min) and V is volume (ml).

(iv) DIP uptake kinetics

The calculated uptake rates v and the DIP concentration (S) in the mixed solution after the DIP spike were used in the Michaelis–Menten equation [22] modified with incorporation of cellular P quotas [11]:

$$v = v_{max} \cdot \frac{S}{K_v + S} \cdot \frac{Q_{max} - Q}{Q_{max} - Q_{min}}, \tag{2.7}$$

where v_{max} is the maximum uptake rate (pmol P ml^{-1} min^{-1}), K_v is the half saturation constant at $0.5v_{max}$ (mg l^{-1}). Q is the instantaneous cellular-nutrient quota, i.e. cellular P quota of the culture when running the bioassays. This Q was approximated from the measured particulate nutrients (see 'Sample analysis'). Q_{max} and Q_{min} are the maximum and minimum cellular-nutrient quotas, respectively. In this study, Q_{max} and Q_{min} were expanded as 1- to 1.5-fold and 0.5- to 1-fold of the maximum and minimum quotas that we measured from the growth experiment, to reasonably cover their ranges. Monte-Carlo simulations were run to determine the best fit of v_{max} and K_v with the given external DIP supply, based on adjusted R^2. The uptake affinity α, the initial slope of the Michaelis–Menten curve at low substrate concentrations was then calculated as follows:

$$\alpha = \frac{v_{max}}{K_v}. \tag{2.8}$$

Higher values of α indicate greater capacity to take up DIP at low DIP concentrations.

(c) Alkaline phosphatase activity assay

(i) Pilot experiment

Pilot experiment was undertaken (see electronic supplementary material, methods S3), and 37°C was determined as the optimal temperature to run alkaline phosphatase activity (APA) assays. The borate buffer with a pH 9.6, mixed with 1 mol l^{-1} boric acid (Chem-Supply, SA, Australia), and 1 mol l^{-1} sodium hydroxide (Ajax Finechem, NSW, Australia), was used to optimize the pH for the assays. The intervals for subsampling for APA were set at 10 s, 20 s, 1 min, and at increasing intervals for a total of eight time points, following the addition of 1 ml borate buffer and 0.3 ml of a 1 mmol l^{-1} 4-MUP substrate solution (4-methylumbelliferyl phosphate disodium salt, Sigma Aldrich M8168 (Sigma Aldrich, MO, USA), diluted in MilliQ water) into a 2.7 ml subculture.

(ii) Assay set-up and APA measurement

In this study, APA of the whole culture was measured to approximate the intracellular APA, as insignificant amounts of APA have been found to occur in the filtrate (extracellular) compared with the filters (intracellular) [23]. In the assay, subcultures (2.7 ml) were taken on specific days (electronic supplementary material, table S1), incubated at 37°C for 10 min then APA was measured.

The 2.7 ml subculture was mixed with 4-MUP substrate solution and borate buffer as in the pilot experiment, inverted three times to fully mix, and then immediately transferred to a quartz cuvette of a spectrofluorometer (Carly Eclipse Fluorometer, Varian Australia, Victoria, Australia) for readings. The excitation and the emission wavelengths were set at 360 and 440 nm, respectively.

(iii) APA calculation

APA was calculated by comparing the relative fluorescent units against a standard curve using 4-MUF (4-methylumbelliferon

Table 2. Average days to photosynthetic yield reduction (d) for the *R. raciborskii* and *C. ovalisporum* strains under P-free and NP-free treatments.

		time to photosynthetic yield reduction (d)	
species	strain	P-free	NP-free
Raphidiopsis raciborskii	WS01	12	12
	WS02	14	14
	WS03	12	12
	WS08	7	10
	WS09	10	14
	WS11	9	10
Chrysosporum ovalisporum	LHC01	55	21
	LHC02	54	14

sodium salt; Sigma Aldrich M1381, Sigma Aldrich, MO, USA). This standard curve was produced on each day when running the APA assays (see days listed in electronic supplementary material, table S1). The rate of APA was then calculated for each strain from each treatment on these days.

(d) Sample analysis

(i) Growth rate, cell enumeration and biovolume

Subcultures (5 ml) were taken for OD750 readings and cell enumeration two to three times a week until the day of 10% photosynthetic yield reduction (table 2), as per methods in Xiao *et al*. [12]. Our previous studies showed that Australian *R. raciborskii* strains do not have well defined lag, exponential, stationary and decline phases, irrespective of growth media or conditions [12,24–26]. However, for the purpose of this study, we used the first order rate kinetics [26,27] to calculate the growth rate from cell enumeration, and we defined exponential growth phase as corresponding to period before a substantial decrease in growth rate, suggesting that cells were approaching stationary phase and acknowledging that growth rates were not clearly delineated in a classical definition.

Cell width and length, trichome length, cell enumeration and biovolume were measured microscopically for preserved samples, and used to calculate cell volume following Xiao *et al*. [12], Zohary *et al*. [28]. The volume of vegetative cells and heterocysts was computed assuming a cylindrical shape for vegetative cells for both species, and spherical and prolate spheroid shapes for *C. ovalisporum* and *R. raciborskii* heterocysts, respectively [29]. The cell number and volume were determined from measuring one replicate of each strain under each nutrient treatment on each sampling day, and the remaining samples were calculated from the correlation between OD750 and cell counts (electronic supplementary material, table S3). Note that in this study, heterocysts started to differentiate approximately 5 days after N deprivation (data not shown in this study, as it is not the focus).

(ii) Cellular C, N and P, and dissolved inorganic N and P analyses

Particulate C, N and P of all strains under each treatment were taken for analysis at a known volume (listed in electronic supplementary material, table S1) and were used to approximate the cellular content of C, N and P, respectively, as per Xiao *et al*. [12]. Cellular P quota was then determined in three forms: standardizing by cellular P to C (μg P μg^{-1} C), cell number (μg P $cell^{-1}$) and biovolume (μg P μm^{-3}).

Filtrates (12 ml) of each culture were collected by passing samples through 0.45 μm cellulose acetate membrane filters (Sartorius Stedim Biotect, Germany), and DIN (ammonium + nitrate/nitrite) and P (phosphate) concentrations were measured following Xiao *et al*. [12].

(e) Statistical analysis

Differences in exponential growth rates, cellular P quotas (P per unit C, cell and biovolume), maximum DIP uptake rates, and maximum APA, under the three nutrient treatments and for all strains were tested by two-way ANOVA. Data were Boxcox-transformed to meet the assumptions of homogeneity of variances and normal distribution of residuals [30]. Levene's test was run to test the homogeneity of variance, and the Shapiro–Wilk test was used to test for normality of the distribution of residuals. All ANOVA tests were followed with a *post hoc* Tukey's test to determine significant differences ($p < 0.05$) among strains and treatments [31]. All statistical analyses were performed with R software (www.r-.project.org). Segmented regression analysis was used to determine the threshold of cellular P quotas where there was an abrupt change in DIP uptake affinity and APA (R software package: *segmented*).

3. Results

(a) Photosynthetic yield and growth rate

The time for *C. ovalisporum* to reach photosynthetic yield reduction was substantially longer than that of *R. raciborskii* in the P-free treatment (i.e. 7–14 days for the six *R. raciborskii* strains, compared with 54–55 days for the two *C. ovalisporum* strains; table 2; electronic supplementary material, figure S2). The time for yield reduction in *C. ovalisporum* strains was also much longer in the P-free treatment than in the NP-free treatment, but this was not the case for *R. raciborskii* strains (table 2). For nearly all strains across all treatments, photosynthetic yield reduction occurred when cell concentrations increase had slowed or had stopped increasing (electronic supplementary material, figure S2).

The mean exponential growth rate varied by approximately twofold and threefold among *C. ovalisporum* and *R. raciborskii* strains across the three nutrient treatments, respectively, and threefold when combining them all (figure 2). Most strains had significantly lower growth rates in NP-free treatment compared to the P-free and replete DIN and P treatments ($p < 0.05$; figure 2). Four of the strains (WS02, WS09, WS11 and LHC02) always had significantly lower growth rates in the P-free treatment than in the replete DIN and P treatment ($p < 0.05$), while the other strains showed no statistical difference (figure 2).

(b) Cellular-nutrient concentration and stoichiometry

The cellular C, N and P content varied substantially among species, strains, nutrient treatments and over the duration of the growth experiments (electronic supplementary material, table S4). For instance, cellular P content varied by nearly 16- and 17-fold among all strains and all treatments of *R. raciborskii* and *C. ovalisporum*, respectively (electronic supplementary material, table S4). Cellular P quotas mostly decreased under P-free and NP-free treatments but increased under the replete NP treatment, varying by strains. For instance, P quota of *C. ovalisporum* LHC01 decreased by approximately 20-fold during the 55-day experiment in the

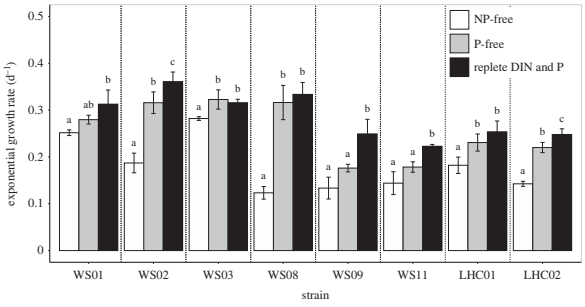

Figure 2. Exponential growth rates of *R. raciborskii* (WS) and *C. ovalisporum* (LHC) strains under the three nutrient treatments; (a, b and c) indicate differences for the same strain among different treatments.

P-free treatment, from 0.075 to 0.004 μg P μg^{-1} C (electronic supplementary material, figure S3*a*).

On the day of photosynthetic yield reduction, cellular P quotas (P per unit C, cell or biovolume), were always significantly higher in replete DIN and P treatments than P-free and NP-free treatments for all strains ($p < 0.05$, electronic supplementary material, figure S4). All the eight strains had higher P quotas in the NP-free treatment than P-free treatment, but were only statistically higher for four strains, WS03, WS08, LHC01 and LHC02 ($p < 0.05$, electronic supplementary material, figure S4).

In the treatments with replete P, irrespective of DIN availability or cell growth stage, *C. ovalisporum* strains always stored significantly more P per unit C or cell than *R. raciborskii* strains, but not necessarily more P per unit biovolume (electronic supplementary material, figure S5). This was evidenced by comparing P quotas between the NP-free treatment on day 0 (when cultures were acclimated to DIN-free condition prior to being inoculated under the NP-free treatment, hence P was replete on the day), and day 0 and the day of photosynthetic yield reduction under the replete DIN and P treatment (electronic supplementary material, figure S5).

(c) Dissolved nutrient concentrations

The ammonium, nitrate/nitrite and DIP concentrations in the growth media varied among strains, nutrient treatments and over the duration of the experiments (electronic supplementary material, table S5). DIP was mostly close to, or below the detection limit of 0.001 mg l^{-1} in P-free and NP-free treatments on the day of photosynthetic yield reduction. When DIN was not supplied, i.e. in the NP free treatment on the day of photosynthetic yield reduction, ammonium and nitrate/nitrite concentrations ranged from 0.009 to 0.027 mg l^{-1} and 0.008 to 0.032 mg l^{-1}, respectively, across all *R. raciborskii* and *C. ovalisporum* strains (electronic supplementary material, table S5).

(d) DIP uptake rates and kinetics

On the day of photosynthetic yield reduction, the measured maximum DIP uptake rates (derived from spiking with the highest concentration of DIP standard solution) varied by fourfold among *C. ovalisporum* strains, and increased to 100-fold when including *R. raciborskii* strains (electronic supplementary material, table S6). The maximum DIP uptake rates were significantly lower in the treatment with replete DIN and P than those in the NP-free and P-free treatment for all strains, but showed no significant difference between NP-free and P-free treatments, except for WS01 and WS11 which were significantly lower in the NP-free treatment (electronic supplementary material, table S6).

DIP uptake kinetics across the four strains used in these experiments (*R. raciborskii* WS02 and WS09, *C. ovalisporum* LHC01 and LHC02) followed Michaelis–Menten kinetics (equation (2.8), incorporating cellular P quotas), irrespective of nutrient treatment or growth stage (figure 3). In figure 3, day 7 from P-free and NP-free treatments was the day during the exponential growth phase; days 10 and 14 from P-free and NP-free treatments were the days of photosynthetic yield reduction and chosen as the late exponential growth phase. To ensure accurate comparisons of DIP uptake kinetics against cellular P quotas with and without DIP supply, samples from the replete DIN and P treatment were supposed to be chosen as days corresponding to photosynthetic yield reduction in either P-free or NP-free treatment (i.e. days 14 for both *R. raciborskii* WS02 and WS09). While, for logistical reasons, day 18 was chosen for WS02, we believed that very minor changes occurred in DIP uptake kinetics and cellular P quotas in WS02 within the 4 days.

Hence, DIP uptake affinity α (v_{max}/K_v) varied across strains, growth stage and treatments. The lowest uptake affinity occurred in the treatment with replete DIN and P for all strains (table 1). *R. raciborskii* WS02 and WS09 both had a higher value of α in the early exponential phase for NP-free treatment, whereas WS09 had a higher α later in the exponential phase (table 1). On the day of photosynthetic yield reduction, the strains of *C. ovalisporum* (LHC01 and LHC02), and *R. raciborskii* WS02 had the highest values of α in the NP-free treatment, while only *R. raciborskii* WS09 had the highest value in the P-free treatment. Some strains showed an abrupt increase in v_{max} under the highest DIP concentration, e.g. WS02 in the NP-free treatment on day 14 had a v_{max} of 1.5 μg P μg^{-1} C d^{-1}, which deviated from the model prediction of approximately 1.2 µg P μg^{-1} C d^{-1} by 20% (electronic supplementary material, figure S6).

Combining α values from the four strains and three nutrient treatments, there was a declining trend with increase in P quota per unit C (figure 4). Considering *R. raciborskii* strains only, DIP uptake rates increased sharply for a quota of less than 0.0098 µg P μg^{-1} C (figure 4).

(e) Alkaline phosphatase activity

APA values varied inconsistently with growth stage of *R. raciborskii* and *C. ovalisporum* strains when DIP supply was absent (electronic supplementary material, figure S7). Therefore, for comparisons between species, strains and treatments, the maximum APA values were used (figures 5 and 6). This APA value varied by approximately 20-fold among *R. raciborskii* strains across the three nutrient treatments, but 60-fold when combining all *R. raciborskii* and *C. ovalisporum* strains. Values of the maximum APA of *C. ovalisporum* strains were significantly higher than that of *R. raciborskii* strains per unit C, cell or biovolume (figure 6). The P-free treatment resulted in significantly higher maximum APA than the replete DIN and P treatment for all strains, and the NP-free treatment for all strains except WS03 ($p < 0.05$; figure 5).

Combining APA from all strains from all nutrient treatments, there was a clear declining trend with increased P quota per unit C (figure 7). At a P quota threshold of

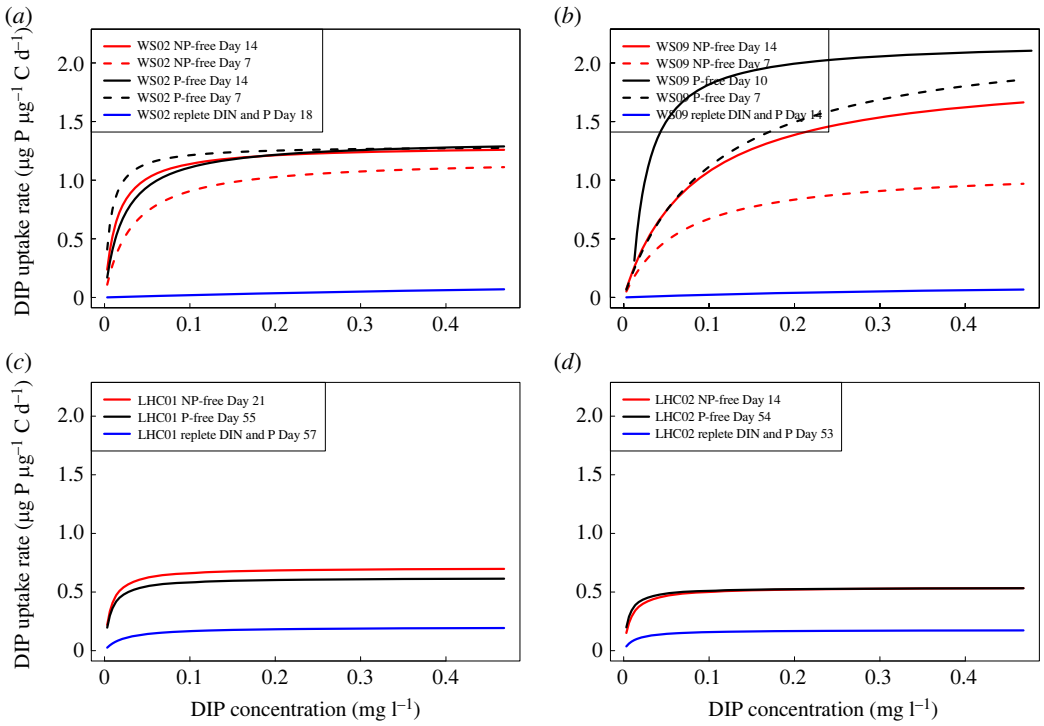

Figure 3. DIP uptake kinetics of *R. raciborskii* strains WS02 and WS09, and *C. ovalisporum* strains LHC01 and LHC02 under the three nutrient treatments on different days. For example, WS02 NP-free day14 in (*a*) means that the bioassay in measuring DIP uptake kinetics was conducted with the culture of *R. raciborskii* strain WS02 grown under NP-free treatment for 14 days. A Michaelis–Menten function was applied for curve fitting.

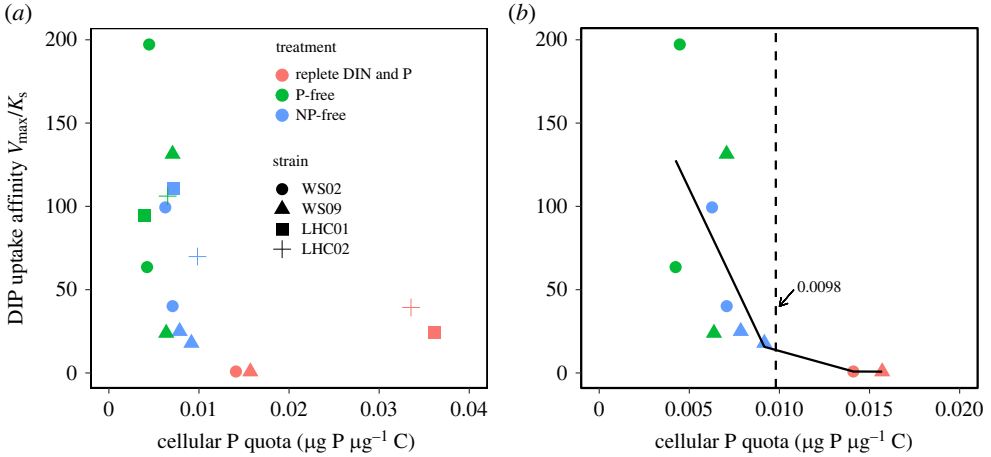

Figure 4. DIP uptake affinity α (v_{max}/K_v) in relation to cellular P quotas for *R. raciborskii* strains WS02 and WS09, and *C. ovalisporum* strains LHC01 and LHC02 under the three nutrient treatments (*a*). Dashed line indicates the threshold of cellular P quota for affinity changes for the two *R. raciborskii* strains through segmented regression analysis (*b*).

approximately 0.0101 μg P μg^{-1} C, APA increased sharply, based on analysis of the strains of the two species either together or separately (figure 7).

4. Discussion

(a) Cellular P storage is critical for DIP uptake and DOP utilization

Our study has shed new light on the critical role of cellular-nutrient storage in determining switches in nutrient utilization strategies, which differ substantially between species and their strains. This study showed that cellular phosphorus (P) storage by the cyanobacteria *R. raciborskii* (basionym *C. raciborskii*) and *C. ovalisporum* (basionym *A. ovalisporum*) is inversely related to uptake affinity α (= maximum uptake rate (v_{max})/ half saturation constant (K_v)) of phosphate (DIP) and APA. A cellular P quota of approximately 0.01 μg P μg^{-1} C delineates a transition between low- and high-affinity of DIP uptake across all six *R. raciborskii* strains. The same threshold also occurred for APA for the *R. raciborskii* strains and two *C. ovalisporum* strains. This threshold was obtained irrespective of external supplies of DIP or dissolved inorganic nitrogen (DIN). Analysis of P quotas needs to become an integral part of physiological studies and models should also include dynamic changes in quotas to improve predictions of cyanobacteria responses to nutrient limitation. This would ultimately affect species competition and dominance under nutrient limitation, and will aid strategies to mitigate cyanobacterial blooms.

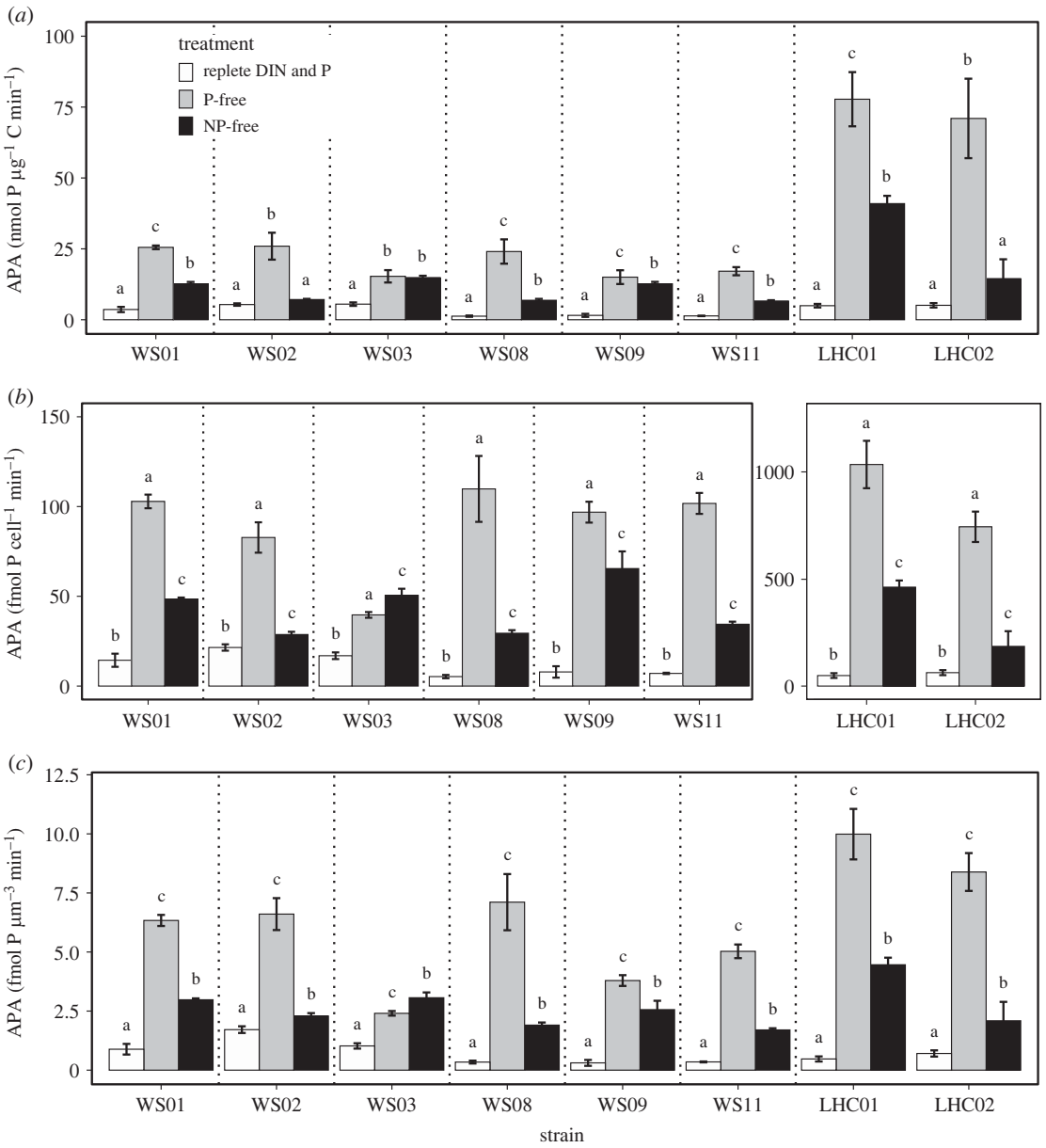

Figure 5. The comparison of maximum APA for each *R. raciborskii* (WS) and *C. ovalisporum* (LHC) strain between treatments of replete DIN and P, P-free and NP-free: (*a*) APA (nmol P µg^{-1} C min^{-1}), (*b*) APA (nmol P cell^{-1} min^{-1}) and (*c*) APA (nmol P µm^{-3} min^{-1}).

DIP uptake kinetics have been extensively studied in laboratory cultures and field populations of cyanobacteria, and either v_{max} or K_v has been used to compare nutrient uptake capacity within and between species [11,32,33]. Our results highlight the inadequacy of using these parameters individually as considerable variability exists in v_{max} and K_v among species, strains and even in the same strain at different growth phases or under different nutrient treatments (see Results) [5]. For example, a study of K_v values for a marine cyanobacterium, *Synechococcus* sp. WH7803 differed by greater than 20-fold between DIP-replete and DIP-starved treatments [33]. v_{max} also increased as DIP supply decreased, indicating the induction of a high-affinity DIP transport system for WH7803 [33]. The same has been found for *R. raciborskii* laboratory cultures and field populations [10,23]. *Synechococcus* PCC6803 has two complete *pstSCAB* systems; one with low uptake affinity but high uptake rate and another with high uptake affinity but low uptake rate, underpinning the independence of v_{max} and K_v [34]. On the other hand, a marine cyanobacterium, *Prochlorococcus*, with low v_{max} measured in laboratory cultures and field populations, can still compete in low DIP environments due to high uptake affinity [35,36]. By contrast, similar K_v values occur for species grown at the same DIP concentration; for example, *R. raciborskii*, *Microcystis aeruginosa* and *Aphanizomenon flos-aquae* [32]. This was also demonstrated for a toxic and non-toxic strain of *M. aeruginosa* [11].

The substantial variation in v_{max} and K_v within and between species could be explained by several factors, including availability and history of nutrients, light and temperature, and cell physiology, e.g. preference for growth versus nutrient storage, and growth phase [37,38]. We recommend using affinity in relation to cellular P quotas, rather than using v_{max} or K_v alone, for a comparison in nutrient utilization capacity, especially under nutrient limiting conditions.

We found APA increased with a decrease in cellular P quotas across strains of *R. raciborskii* and *C. ovalisporum*, similar to findings for *M. aeruginosa* strain 905 [39]. P quotas have also been linked to physiological functions, for example, a study showed that P quota threshold of 0.3–0.45 pg P cell^{-1} was measured for akinete differentiation in trichomes of *Dolichospermum circinale* [40].

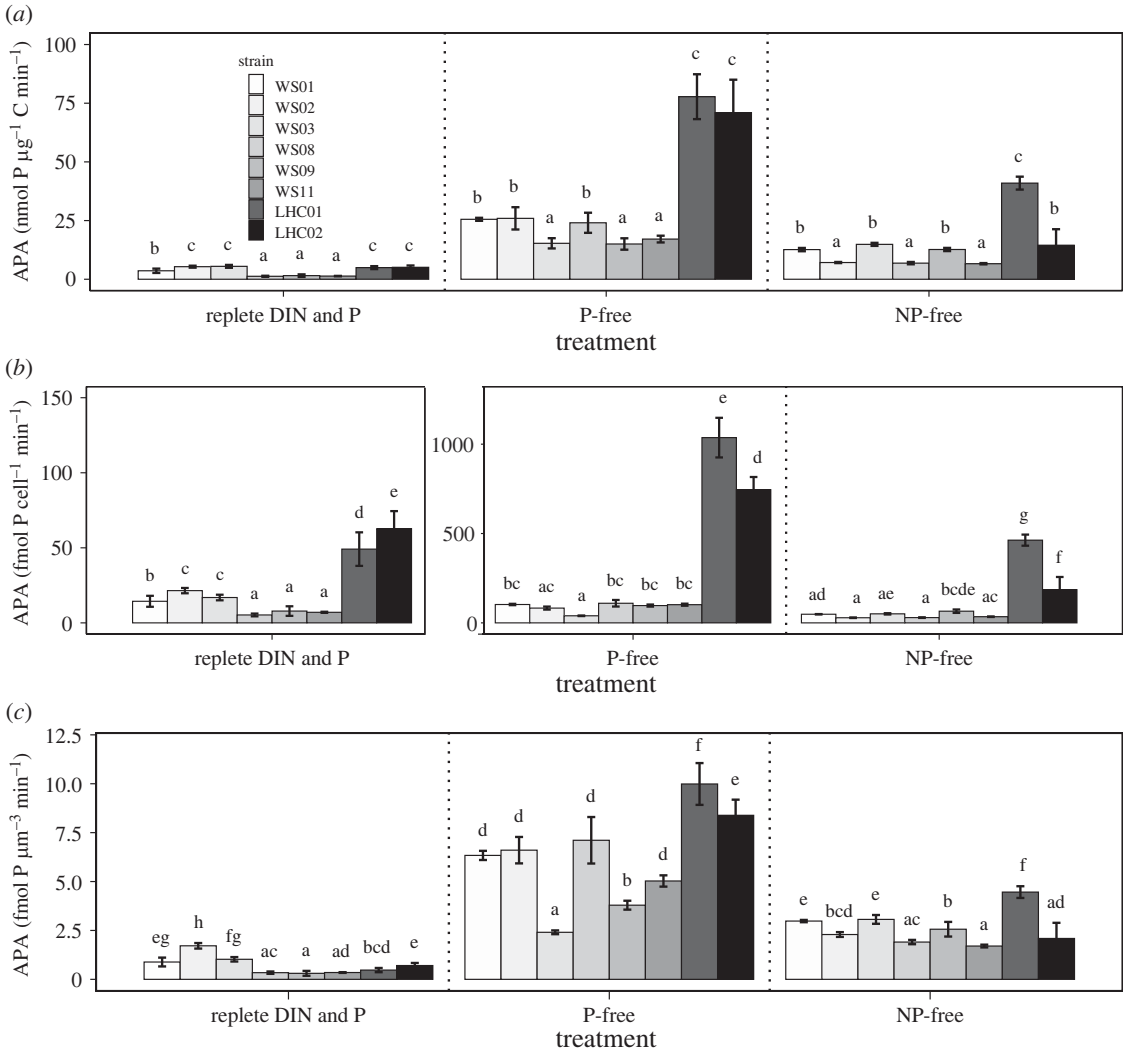

Figure 6. The comparison of maximum APA between *R. raciborskii* (WS) and *C. ovalisporum* (LHC) strains under each of the treatment of replete DIN and P, P-free and NP-free: (*a*) APA (nmol P μg^{-1} C min^{-1}), (*b*) APA (nmol P $cell^{-1}$ min^{-1}) and (*c*) APA (nmol P μm^{-3} min^{-1}).

(b) Inter- and intra-population strain variation

Our study showed that the six *R. raciborskii* strains isolated from one population, and two *C. ovalisporum* strains, isolated from another, varied widely in their exponential growth rates, time to reach photosynthetic yield reduction, cellular-nutrient quotas, DIP uptake rates and APA, in response to treatments with or without DIP and DIN. This substantial inter- and intra-population variability has previously been reported in cyanobacteria responses to different light, temperature and nutrient treatments [12,41]. Strain variability appears to confer resilience of species through flexibility to respond to a wide range of, as well as changing, environmental conditions.

Our study found that under P-free conditions, *C. ovalisporum* cultures maintained their growth for approximately 55 days until P starvation, based on photosynthetic yield reduction. This time was significantly longer than that of *R. raciborskii* strains (less than or equal to 14 days) (see Results and Xiao *et al.* [12]). This could possibly be explained by the significantly higher APA and higher P quotas of *C. ovalisporum* strains than *R. raciborskii* strains. This means that *C. ovalisporum* has greater capacity than *R. raciborskii* to withstand DIP starvation by depleting the P reserves within cells, and using recycled DOP. It should be acknowledged that APA has been interpreted as an indirect proxy for utilization of DOP, the AP enzyme only mineralizes the most abundant and labile constituents of cellular DOP pool, i.e. esters. *R. raciborskii* has also been shown to use other forms of DOP, e.g. phosphonates [23], and it is not clear whether *C. ovalisporum* has this same capacity. However, the utilization of forms of DOP other than esters was not examined in this study.

Schoffelen *et al.* [16] compared the effectiveness of DOP utilization between *C. ovalisporum* and another ubiquitous bloom-forming cyanobacterium, *Dolichospermum*, in field populations when DIP concentrations were very low in summer. The authors found that *C. ovalisporum* acquired approximately 85% of its cellular P-demand from DOP, and only 15% from DIP; while *Dolichospermum* typically obtained 40% of cellular P from DOP, and 60% from DIP. Overall, it appears that *C. ovalisporum* competes strongly for DOP compared with other cyanobacterial species, hence may give it the capacity to dominate phytoplankton populations when DIP becomes limited. Chen *et al.* [42] found that another cyanobacterium, *Aphanizomenon flos-aquae* could maintain growth from a one-off DOP supply for approximately 60 days via APA. The authors concluded that the coordination of dissolved DOP mineralization and continuous utilization of polyphosphate (a typical form of cellular P) might contribute to the maintenance of *A. flos-aquae* when relying on DOP. This time period of 60 days is similar to the time for maintaining growth by *C. ovalisporum* strains in our cultures (approx. 55

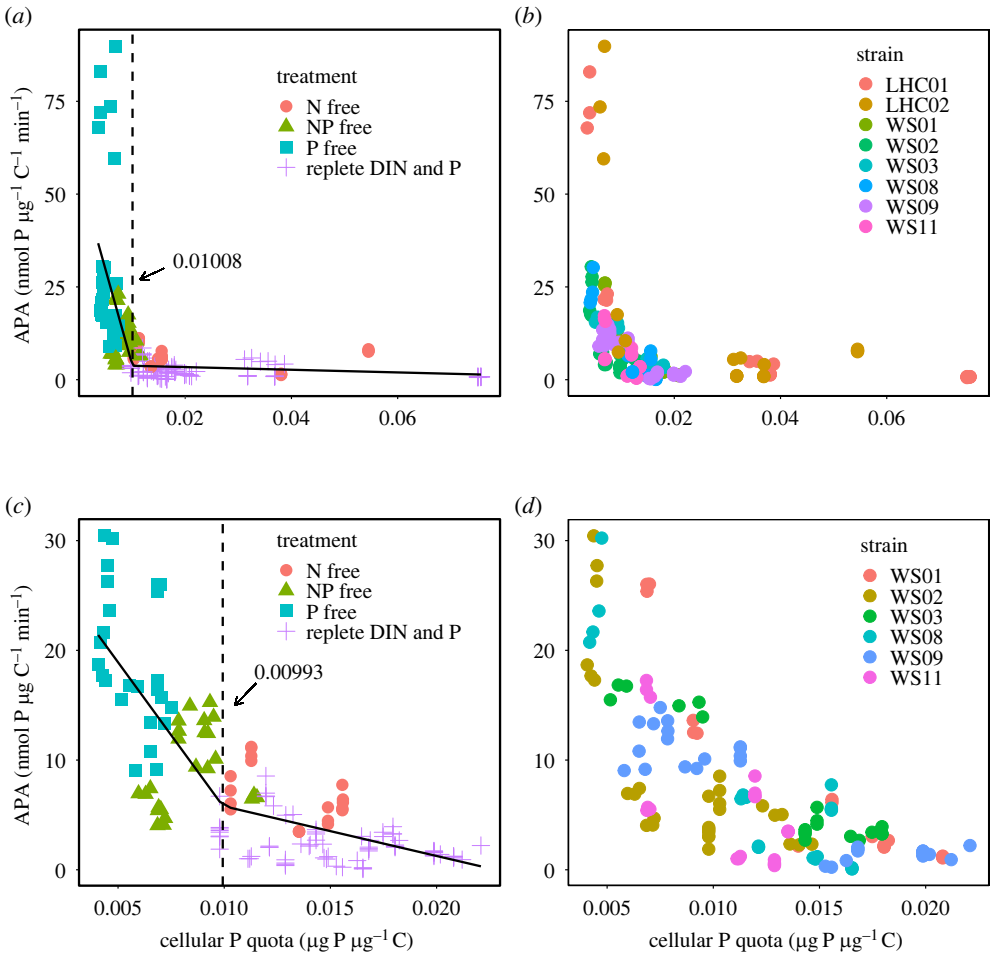

Figure 7. APA of *R. raciborskii* (WS) and *C. ovalisporum* (LH) strains under the three nutrient treatments (N-free indicates the day 0 of NP-free treatment). Dashed lines indicate the threshold of cellular P quota relative to APA change for all the strains combined (*a*,*c*) and *R. raciborskii* strains only (*b*,*d*) through segmented regression analysis.

days), suggesting similarities in the strategies of *Aphanizomenon* and *C. ovalisporum*.

Active uptake of DIP and DOP requires more energy than passive DIP uptake [43], which may necessitate trade-offs between energy investment in the respective form that is taken up. The species *R. raciborskii* appears to be a superior competitor for low concentrations of DIP, while *C. ovalisporum* is a superior competitor for DOP. Hence, *R. raciborskii* may dominate over *C. ovalisporum* when there are frequent spikes of low concentrations of DIP [44], while *C. ovalisporum* could dominate over *R. raciborskii* when DOP is abundant. It should also be noted that in a system with limited DIP input, the hydrolysis of DOP into DIP by *C. ovalisporum* could favour the persistence and coexistence of other species. For instance, Schoffelen *et al.* [16] reported that the capacity of *Aphanizomenon* to use DOP favoured the persistence of *Nodularia*, *Dolichospermum* and *Aphanizomenon* through resource (P) partitioning.

(c) Impact of DIN limitation on P utilization strategies

Our experiments showed that DIN availability affected DIP uptake affinity. In the P-free treatment, DIP uptake affinity of *R. raciborskii* WS02 decreased in the late exponential growth stage, while it increased for WS09. In comparison, for the NP-free treatment, DIP uptake affinity of both strains increased from the early to late exponential growth stages. Therefore, the limitation of DIN reduced the strain variability in terms of their capacity to take up DIP.

We found that three out of the four strains (i.e. *R. raciborskii* WS02, and *C. ovalisporum* LHC01 and LHC02) had lower DIP uptake affinity in the P-free treatment than in the NP-free treatment on the day of photosynthetic yield reduction. The lower uptake affinity in the P-free treatment may be due to insufficient cellular P stores to provide energy for DIP uptake.

(d) Future research

Our culture study highlighted how cellular P quotas and external DIN and P supplies, affect DIP uptake and APA across two diazotrophic cyanobacteria species and multiple strains, emphasizing the importance of measuring cellular P in studying species competition and dominance, especially when DIP is limiting. Therefore, it would be invaluable to replicate these experiments with field population. One previous field study during a *R. raciborskii* bloom, showed that the APA of the population increased dramatically below a threshold of cellular P quota of 0.65 µg P µg^{-1} chlorophyll *a* Prentice *et al.* [45]. Using a C:chlorophyll mass conversion factor of 50:1, this value can be converted to 3.25 µg P µg^{-1} C. However, it should be acknowledged that, this conversion factor can vary by an order of magnitude, depending on species and environmental conditions [46]. This threshold is considerably higher than that of 0.01 µg P µg^{-1} C derived in our study. It highlights the need for a more accurate way of measuring P quotas in individual cyanobacterial species or strains and to

reduce potential confounding effects from other phytoplankton, bacteria, viruses, detritus, and inorganic material.

In this study, batch cultures were used and using pre-starving of cells and regular monitoring of photosynthetic yield, P limitation could be determined. However, future studies would benefit from continuous culture experiments which would allow manipulation of a range of DIP concentrations. We have made it clear that DIP uptake kinetics would change substantially with different nutrient treatments and sampling days from the two *R. raciborskii* strains. We acknowledge that we have not fully quantified population variability and that this should be a focus of future studies.

Our study found multi-phasic uptake kinetics in P-free treatment, with uptake rates of DIP increased again after reaching a plateau, suggesting activation of one or more nutrient transport systems with increasing DIP inputs. This multi-phasic rather than monophasic uptake kinetics has been shown in the uptake rates of N or P in a number of phytoplankton species [47,48]. There is a challenge now to improve models by incorporating multi-phasic uptake kinetics, which may be particularly important for replenishment of cyanobacteria nutrient quotas when there are intermittent pulses of nutrients (e.g. from stormflows and mixing events [49]).

5. Conclusion

Our study, using strains from two diazotrophic cyanobacterial species, *R. raciborskii* and *C. ovalisporum*, provides evidence that cellular P quota drives high-affinity DIP uptake and APA at a critical threshold of approximately 0.01 µg P µg^{-1} C. *R. raciborskii* has superior DIP uptake rates, while *C. ovalisporum* has superior APA capacity under low DIP concentrations. Hence there is a trade-off between DIP uptake and DOP utilization when DIP supply is limited. Further limitation by DIN, forcing N fixation to occur, accelerates DIP uptake in both species and reduces the intra-population variability in DIP uptake and APA. This study builds on our previous understanding of intra-population variation in P allocation to growth and storage in cyanobacteria, shedding new light on extreme strategies of DIP uptake and APA in two species, and suggests that P reduction strategies may not prove to be effective immediately for species that are well adapted to low-P conditions because of high internal storage capacity.

Data accessibility. Codes, data and metadata to support the manuscript are available on Dryad [50].

Supplementary material is available online [51].

Authors' contributions. M.X.: conceptualization, data curation, formal analysis, funding acquisition, investigation, methodology, writing—original draft and writing—review and editing; M.A.B.: conceptualization, funding acquisition, project administration, resources, supervision and writing—review and editing; M.J.P.: data curation, methodology and writing—review and editing; E.F.G.: data curation, methodology and writing—review and editing; A.C.: data curation, methodology and writing—review and editing; D.P.H.: conceptualization, funding acquisition, project administration, resources, supervision and writing—review and editing.

All authors gave final approval for publication and agreed to be held accountable for the work performed therein.

Conflict of interest declaration. The authors declare no competing interests.

Funding. This work was supported by Australian Research Council [ARC Discovery Project DP2209560] to DPH and MAB; Griffith Sciences New Researcher Grant, National Key R&D Program of China [2022YFC3203605-01] and Science and Technology Planning Project of NIGLAS [NIGLAS2022TJ08] to MX; and the Coordenação de Aperfeiçoamento de Pessoal de Nível Superior for PhD scholarship 001 to EFG.

Acknowledgements. We thank Sian Taylor for helping with the experimental work. We also thank the editors and reviewers for their careful reviews of the manuscript.

References

1. Conley DJ, Paerl HW, Howarth RW, Boesch DF, Seitzinger SP, Havens KE, Lancelot C, Likens GE. 2009 Controlling eutrophication: nitrogen and phosphorus. *Science* **323**, 1014–1015. (doi:10.1126/science.1167755)
2. Burford MA, Willis A, Xiao M, Prentice MJ, Hamilton DP. 2023 Understanding the relationship between nutrient availability and freshwater cyanobacterial growth and abundance. *Inland Waters* 1–24. (doi:10.1080/20442041.2023.2204050)
3. Freeman EC, Creed IF, Jones B, Bergström AK. 2020 Global changes may be promoting a rise in select cyanobacteria in nutrient-poor northern lakes. *Glob. Chang. Biol.* **26**, 4966–4987. (doi:10.1111/gcb.15189)
4. Burford MA, Beardall J, Willis A, Orr PT, Magalhaes VF, Rangel LM, Azevedo SM, Neilan BA. 2016 Understanding the winning strategies used by the bloom-forming cyanobacterium *Cylindrospermopsis raciborskii*. *Harmful Algae* **54**, 44–53. (doi:10.1016/j.hal.2015.10.012)
5. Xiao M, Burford MA, Wood SA, Aubriot L, Ibelings B, Prentice M, Galvanese E, Harris TD, Hamilton DP. 2022 Schindler's legacy: from eutrophic lakes to the phosphorus utilization strategies of cyanobacteria. *FEMS Microbiol. Rev.* **46**, fuac029. (doi:10.1093/femsre/fuac029)
6. Lin S, Litaker RW, Sunda WG. 2016 Phosphorus physiological ecology and molecular mechanisms in marine phytoplankton. *J. Phycol.* **52**, 10–36. (doi:10.1111/jpy.12365)
7. Xiao M, Hamilton DP, O'Brien KR, Adams MP, Willis A, Burford MA. 2020 Are laboratory growth rate experiments relevant to explaining bloom-forming cyanobacteria distributions at global scale? *Harmful Algae* **92**, 101732. (doi:10.1016/j.hal.2019.101732)
8. Lei L, Peng L, Huang X, Han B. 2014 Occurrence and dominance of *Cylindrospermopsis raciborskii* and dissolved cylindrospermopsin in urban reservoirs used for drinking water supply, South China. *Environ. Monit. Assess.* **186**, 3079–3090. (doi:10.1007/s10661-013-3602-8)
9. Burford MA, O'Donohue MJ. 2006 A comparison of phytoplankton community assemblages in artificially and naturally mixed subtropical water reservoirs. *Freshwater Biol.* **51**, 973–982. (doi:10.1111/j.1365-2427.2006.01536.x)
10. Prentice MJ, Brien KR, Hamilton DP, Burford MA. 2015 High- and low-affinity phosphate uptake and its effect on phytoplankton dominance in a phosphate-depauperate lake. *Aquat. Microb. Ecol.* **75**, 139–153. (doi:10.3354/ame01751)
11. Suominen S, Brauer VS, Rantala-Ylinen A, Sivonen K, Hiltunen T. 2017 Competition between a toxic and a non-toxic *Microcystis* strain under constant and pulsed nitrogen and phosphorus supply. *Aquat. Ecol.* **51**, 117–130. (doi:10.1007/s10452-016-9603-2)
12. Xiao M, Hamilton DP, Chuang A, Burford MA. 2020 Intra-population strain variation in phosphorus storage strategies of the freshwater cyanobacterium *Raphidiopsis raciborskii*. *FEMS Microbiol. Ecol.* **96**, fiaa092. (doi:10.1093/femsec/fiaa092)
13. Wetzel RG. 2001 *Limnology: lake and river ecosystems*, 3rd edition. San Diego, CA: Academic Press.
14. Lu Z, Lei L, Lu Y, Peng L, Han B. 2021 Phosphorus deficiency stimulates dominance of *Cylindrospermopsis* through facilitating cylindrospermopsin-induced alkaline phosphatase secretion: Integrating field and laboratory-based evidences. *Environ. Pollut* **290**, 117946. (doi:10.1016/j.envpol.2021.117946)
15. Bai F, Liu R, Yang Y, Ran X, Shi J, Wu Z. 2014 Dissolved organic phosphorus use by the invasive freshwater diazotroph cyanobacterium,

Cylindrospermopsis raciborskii. *Harmful Algae* **39**, 112–120. (doi:10.1016/j.hal.2014.06.015)

16. Schoffelen NJ, Mohr W, Ferdelman TG, Littmann S, Duerschlag J, Zubkov MV, Ploug H, Kuypers MMM. 2018 Single-cell imaging of phosphorus uptake shows that key harmful algae rely on different phosphorus sources for growth. *Sci. Rep.* **8**, 17182. (doi:10.1038/s41598-018-35310-w)
17. Aubriot L. 2019 Nitrogen availability facilitates phosphorus acquisition by bloom-forming cyanobacteria. *FEMS Microbiol. Ecol.* **95**, fiy229. (doi:10.1093/femsec/fiy229)
18. Orchard ED, Webb EA, Dyhrman ST. 2009 Molecular analysis of the phosphorus starvation response in *Trichodesmium* spp. *Environ. Microbiol.* **11**, 2400–2411. (doi:10.1111/j.1462-2920.2009.01968.x)
19. Burford M, Hamilton D, Yu S, Chuang A, Faggotter S, Frassl M. 2020 *Trialling possible scenarios to assess potential options for reducing the frequency and duration of cyanobacteria blooms in Lake Hugh Muntz*. Brisbane, Australia: Australian Rivers Institute, Griffith University.
20. Willis A, Adams MP, Chuang AW, Orr PT, O'Brien KR, Burford MA. 2015 Constitutive toxin production under various nitrogen and phosphorus regimes of three ecotypes of *Cylindrospermopsis raciborskii* ((Wołoszyńska) Seenayya et Subba Raju). *Harmful Algae* **47**, 27–34. (doi:10.1016/j.hal.2015.05.011)
21. Franklin HM, Garzon-Garcia A, Burton J, Moody PW, De Hayr RW, Burford MA. 2018 A novel bioassay to assess phytoplankton responses to soil-derived particulate nutrients. *Sci. Total Environ.* **636**, 1470–1479. (doi:10.1016/j.scitotenv.2018.04.195)
22. Michaelis L, Menten ML. 1913 Die kinetik der invertinwirkung. *Biochem z* **49**, 333–369.
23. Willis A, Chuang A, Dyhrman S, Burford M. 2019 Differential expression of phosphorus acquisition genes in response to phosphorus stress in two *Raphidiopsis raciborskii* strains. *Harmful Algae* **82**, 19–25. (doi:10.1016/j.hal.2018.12.003)
24. Willis A, Ind A, Burford M. 2017 Variations in carbon-to-phosphorus ratios of two Australian strains of *Cylindrospermopsis raciborskii*. *Eur. J. Phycol.* **52**, 1–8. (doi:10.1080/09670262.2017.1286524)
25. Pierangelini M, Sinha R, Willis A, Burford M, Orr PT, Beardall J, Neilan BA. 2015 Constitutive cylindrospermopsin cellular pool size in *Cylindrospermopsis raciborskii* under different light and pCO_2 conditions. *Appl. Environ. Microbiol.* **81**, 3069–3076. (doi:10.1128/AEM.03556-14)
26. Xiao M, Willis A, Burford MA. 2017 Differences in cyanobacterial strain responses to light and temperature reflect species plasticity. *Harmful Algae* **62**, 84–93. (doi:10.1016/j.hal.2016.12.008)
27. Andersen RA. 2005 *Algal culturing techniques*. London, UK: Academic press.
28. Zohary T, Shneor M, Hambright KD. 2016 PlanktoMetrix - a computerized system to support microscope counts and measurements of plankton. *Inland Waters* **6**, 131–135. (doi:10.5268/IW-6.2.965)
29. Hillebrand H, Dürselen CD, Kirschtel D, Pollingher U, Zohary T. 1999 Biovolume calculation for pelagic and benthic microalgae. *J. Phycol.* **35**, 403–424. (doi:10.1046/j.1529-8817.1999.3520403.x)
30. Zuur AF, Ieno EN, Elphick CS. 2010 A protocol for data exploration to avoid common statistical problems. *Methods Ecol. Evol.* **1**, 3–14. (doi:10.1111/j.2041-210X.2009.00001.x)
31. Day RW, Quinn GP. 1989 Comparisons of treatments after an analysis of variance in ecology. *Ecol. Monogr.* **59**, 433–463. (doi:10.2307/1943075)
32. Wu Z, Shi J, Li R. 2009 Comparative studies on photosynthesis and phosphate metabolism of *Cylindrospermopsis raciborskii* with *Microcystis aeruginosa* and *Aphanizomenon flos-aquae*. *Harmful Algae* **8**, 910–915. (doi:10.1016/j.hal.2009.05.002)
33. Donald KM, Scanlan DJ, Carr NG, Mann NH, Joint I. 1997 Comparative phosphorus nutrition of the marine cyanobacterium *Synechococcus* WH7803 and the marine diatom *Thalassiosira weissflogii*. *J. Plankton Res.* **19**, 1793–1813. (doi:10.1093/plankt/19.12.1793)
34. Pitt FD, Mazard S, Humphreys L, Scanlan DJ. 2010 Functional characterization of *Synechocystis* sp. strain PCC 6803 *pst1* and *pst2* gene clusters reveals a novel strategy for phosphate uptake in a freshwater cyanobacterium. *J. Bacteriol.* **192**, 3512–3523. (doi:10.1128/JB.00258-10)
35. Casey JR, Lomas MW, Michelou VK, Dyhrman ST, Orchard ED, Ammerman JW, Sylvan JB. 2009 Phytoplankton taxon-specific orthophosphate (Pi) and ATP utilization in the western subtropical North Atlantic. *Aquat. Microb. Ecol.* **58**, 31–44. (doi:10.3354/ame01348)
36. Krumhardt KM, Callnan K, Roache-Johnson K, Swett T, Robinson D, Reistetter EN, Saunders JK, Rocap G, Moore LR. 2013 Effects of phosphorus starvation versus limitation on the marine cyanobacterium *Prochlorococcus* MED4 I: uptake physiology. *Environ. Microbiol.* **15**, 2114–2128. (doi:10.1111/1462-2920.12079)
37. Jansson M. 1988 Phosphate uptake and utilization by bacteria and algae. Hydrobiologia **170**, 177–189. (doi:10.1007/BF00024904)
38. Ritchie RJ, Trautman DA, Larkum AWD. 2001 Phosphate limited cultures of the cyanobacterium *Synechococcus* are capable of very rapid, opportunistic uptake of phosphate. *New Phytol.* **152**, 189–201. (doi:10.1046/j.0028-646X.2001.00264.x)
39. Zheng Y, Mi W, Bi Y, Hu Z. 2017 The response of phosphorus uptake strategies of *Microcystis aeruginosa* to hydrodynamics fluctuations. *Environ. Sci. Pollut. Res.* **24**, 9251–9258. (doi:10.1007/s11356-017-8502-y)
40. Van Dok W, Hart BT. 1996 Akinete differentiation in *Anabaena circinalis* (Cyanophyta). *J. Phycol.* **32**, 557–565. (doi:10.1111/j.0022-3646.1996.00557.x)
41. Guedes IA, Pacheco ABF, Vilar MCP, Mello MM, Marinho MM, Lurling M, Azevedo SMFO. 2019 Intraspecific variability in response to phosphorus depleted conditions in the cyanobacteria *Microcystis aeruginosa* and *Raphidiopsis raciborskii*. *Harmful Algae* **86**, 96–105. (doi:10.1016/j.hal.2019.03.006)
42. Chen X *et al.* 2020 Strategies adopted by *Aphanizomenon flos-aquae* in response to phosphorus deficiency and their role on growth. *Environ. Sci. Eur.* **32**, 1–13. (doi:10.1186/s12302-020-00328-3)
43. Falkowski PG, Raven JA. 2013 *Aquatic photosynthesis*. Princeton, NJ: Princeton University Press.
44. Amaral V, Bonilla S, Aubriot L. 2014 Growth optimization of the invasive cyanobacterium *Cylindrospermopsis raciborskii* in response to phosphate fluctuations. *Eur. J. Phycol.* **49**, 134–141. (doi:10.1080/09670262.2014.897760)
45. Prentice MJ, Hamilton DP, Willis A, O'Brien KR, Burford MA. 2019 Quantifying the role of organic phosphorus mineralisation on phytoplankton communities in a warm-monomictic lake. *Inland Waters* **9**, 10–24. (doi:10.1080/20442041.2018.1538717)
46. Yacobi Y, Zohary T. 2010 Carbon:Chlorophyll a ratio, assimilation numbers and turnover times of Lake Kinneret phytoplankton. *Hydrobiologia* **639**, 185–196. (doi:10.1007/s10750-009-0023-3)
47. Glibert PM, Wilkerson FP, Dugdale RC, Raven JA, Dupont CL, Leavitt PR, Parker AE, Burkholder JM, Kana TM. 2016 Pluses and minuses of ammonium and nitrate uptake and assimilation by phytoplankton and implications for productivity and community composition, with emphasis on nitrogen-enriched conditions. *Limnol. Oceanogr.* **61**, 165–197. (doi:10.1002/lno.10203)
48. Chisholm S, Stross R. 1976 Phosphate uptake kinetics in *Euglena Gracilis* (Z) (Euglenophyceae) grown in light/dark cycles. ii. phased PO_4-limited cultures. *J. Phycol.* **12**, 217–222. (doi:10.1111/j.1529-8817.1976.tb00505.x)
49. Wood S, Borges H, Puddick J, Biessy L, Atalah J, Hawes I, Dietrich D, Hamilton D. 2017 Contrasting cyanobacterial communities and microcystin concentrations in summers with extreme weather events: insights into potential effects of climate change. *Hydrobiologia* **785**, 71–89. (doi:10.1007/s10750-016-2904-6)
50. Xiao M, Burford MA, Prentice MJ, Galvanese EF, Chuang A, Hamilton DP. 2023 Data from: Phosphorus storage and utilization strategies of two bloom-forming freshwater cyanobacteria. Dryad Digital Repository. (doi:10.5061/dryad.4f4qrfjhx)
51. Xiao M, Burford MA, Prentice MJ, Galvanese EF, Chuang A, Hamilton DP. 2023 Phosphorus storage and utilization strategies of two bloom-forming freshwater cyanobacteria. Figshare. (doi:10.6084/m9.figshare.c.6729669)